International Journal of Heat and Technology
Vol. 39, No. 4, August, 2021, pp. 1365-1371
Journal homepage: http://iieta.org/journals/ijht

Characterization of a Closed Loop Pulsating Heat Pipe Using Ethanol with Different Angles

Israa S. Ahmed[1], Hussain S. Abd[1], Ayad M. Al Jubori[2*]

[1] Electromechanical Engineering Department, University of Technology, Baghdad, P.O. Box 19006, Iraq
[2] Communication Engineering Department, University of Technology, Baghdad, P.O. Box 19006, Iraq

Corresponding Author Email: ayad.m.salman@uotechnology.edu.iq

https://doi.org/10.18280/ijht.390437

Received: 6 November 2020
Accepted: 2 July 2021

Keywords:
measurement, orientations, pulsating heat pipe, thermal characteristics, two-phase flow

ABSTRACT

In low-temperature difference, a closed-loop pulsating heat pipe (CLPHP) can be used as a cooling device due to its capability to transfer heat. The thermal performance of the CLPHP is affected by the working fluids. In this work, the effects of some operating parameters such as using ethanol as working fluid with 0.5 filling ratio, orientation, and power inputs are offered based on experimental study. Where the CLPHP was constructed and tested to achieve a better vision into the effect of orientation of 0°, 15°, 30°, 45°, and 90°, and power input of 50 W, 115 W, 215 W, and 450 W on the heat transfer characteristics and the thermal performance. The results indicated that the minimum thermal resistance can be reached at 0.1585 (℃/W) with an orientation of 90° and a power input of 450 W. The results revealed that the inclination angles and power inputs had considerable influence on the enhancement of the thermal performance of the CLPHP. For the low boiling temperature of the working fluid, the power input is more favorable because of fast startup compared with a high power input that leads to some difficulties like the dry-out phenomenon.

1. INTRODUCTION

Recently, producing eco-friendly and sustainable energy sources and managing; it is required to effectively solve the energy crisis. Moreover, the researchers wrestle with time to develop sufficient and sustainable energy sources. Therefore, the closed-loop pulsating heat pipe (CLPHP) has acquired/obtained more attention as a possible heat management device that is compact, efficient, passive, and yet simple. Also, it can tackle high-temperature issues in electronic devices. The CLPHP is a passive heat transfer device/system that was developed in many more applications such as electronic cooling, solar cells, automotive technology, etc.

The thermal performance of the thermosiphon and heat pipe as a conventional heat pipe are widely investigated under different operating conditions. Where the effect of the working fluids has been investigated to improve the heat transfer characteristic of the thermosiphon heat pipe as reported in ref. [1-6]. Moreover, some studies focused on the filling ratios, orientation, and nao-fluid technique to achieve a better performance of the conventional heat pipes and thermosiphons [7-9].

The working fluid can be one of the significant parameters that have an influence on the thermal performance of the CLPHP. Several studies have been carried out an experiment to examine the impact of the working fluids. Xu et al. [10] used a mixture of water and HFE-7100 as a working fluid to investigate the heat transfer performance of the pulsating heat pipe. Where different ratios of the volume mixing were investigated namely: 1:4, 1:2, 1:1, 2:1, and 4:1 with a filling ratio of 50%. The minimum thermal resistance of 0.1634 ℃/W at a mixing ratio of 1:2. Xu et al. [11] conducted an experimental investigation of the PHP performance with the ethanol-water mixture as a hybrid working fluid. The best performance was obtained at a mixing ratio of 30% (ethanol-water). Kim, J. and Kim, S.J. [12] experimented with the micro PHP performance using different working fluids. They found that the thermal resistance reduced significantly with ethanol as a working fluid compared with others. Han et al. [13] presented an experimental study on the PHP thermal performance with binary zoetropes' fluids at a vertical orientation. The large filling ratio and high heat load led to reducing PHP performance. Perna et al. [14] characterized the wavelet analysis of the PHP performance with FC-72 (50% vol.) as a working fluid. The results showed that the mean velocity of the flow increased with increasing the heat input. Wu et al. [15] designed and manufactured a PHP for cooling a cutting tool. The PHP was filled with 50% acetone. They found that by using a PHP as a cooling device, their lives were improved 20-30%. Ishii and Fumoto [16] experimentally visualized the temperature distribution inside a PHP, where the temperature distribution was measured utilizing temperature-sensitive paint. The accuracy of temperature measurement was about 0.263℃.

Takawale et al. [17] experimentally studied the performance comparison between the flat plate PHP and the capillary tube at different heat inputs. They pointed that the decrease in the thermal resistance with flat plate PHP was 83% compared to 35% for capillary tube PHP. Kazemi-Beydokhti et al. [18] investigated the impact of nano-complexes on a PHP performance by measuring the synthesized nano-fluids thermal conductivity. Their results showed that the thermal performance of the PHP was enhanced by about 27% using the nano-fluids. Wang et al. [19] numerically investigated the thermal performance of the PHP charged with deionized water.

The thermal resistance was reduced by 10.8% with super-hydrophilic at heat input 20 W. Liang et al. [20] experimented the performance of a close-loop PHP with different mixing volume ratios of acetone and ethanol. The optimum thermal performance was achieved at a mixing volume ratio of 1:6 of ethanol and acetone at a vertical orientation.

From the aforementioned studies related to the CLPHP, it revealed that the preceding studies have mostly focused on using a mixture of working fluid or nano-fluids to enhance the PHP thermal performance. But, limited studies have been reported on the heat transfer characteristics and the closed-loop PHP performance at various working parameters such as fill ratios, orientations, and power inputs. Therefore, in this work, a closed-loop PHP is designed and manufactured to experiment at different orientation angles and power inputs charged with ethanol as a working fluid. Moreover, the CLPHP is manufactured with two turns and tested under start-up conditions that differ from the conventional configurations.

2. EXPERIMENTAL APPARATUS AND PROGRESSION

2.1 Closed loop PHP

In this experimental investigation, the PHP was designed and manufactured with two turns, as displayed in Figure 1. Where the PHP tube was made-up from copper with a total length of 500 mm (evaporator length of 200 mm, adiabatic length of 100 mm, and a condenser length of 200 mm). The bend radius was 7.5 mm with a space of 15 mm between the centers of the two adjacent pipes. Where the critical inner diameter was calculated according to Eq. (1) [21]:

$$D_C = 2\sqrt{\frac{\sigma}{g(\rho_l - \rho_v)}} \quad (1)$$

The PHP internal diameter should be less than the critical diameter of the working fluid to ensure that the accurate physical behavior of the working fluid was achieved in the pulsating condition/status. The correct critical diameter guarantees the prevention of phase separation initiated by vapor bubbles and liquid slugs' accumulation [22]. The PHP design specification is listed in Table 1.

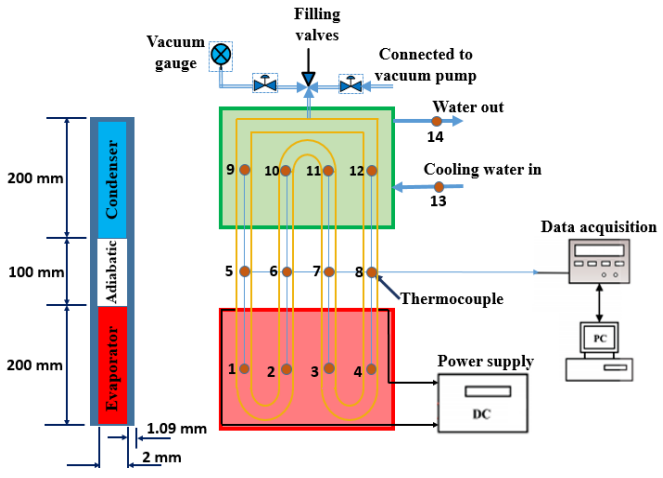

Figure 1. The developed PHP sample

Table 1. The specification, dimensions, and physical properties of the designed PHP

Parameters/Property and Units	Values
Inner diameter (mm)	2
Wall thickness (mm)	1.09
Length of evaporator (mm)	200
Length of adiabatic section (mm)	100
Length of condenser (mm)	200
Thermal conductivity of wall ($W.m^{-1}.K^{-1}$)	401
Number of bends	3
Material	Copper

2.2 Experimental setup

Figure 1 displays the developed experimental rig comprising of: the PHP, the electric heater, evacuating and charging system, water cooling system, and multi-channels acquisition data system. As shown in Figure 1, the CLPHP system consists from four bended pipes with the evaporator part at the lower and a condenser part at the upper. Figure 2 shows a photograph of the developed test device.

The PHP was charged with an ethanol solution as a working fluid by 50% of the total evaporator volume. Moreover, the plug tube allowed access to the inside of the CLPHP after the construction, cleaning, and evacuation using a vacuum pump. The CLPHP was cleaned and evacuated before another working fluid was charged. All parts of the PHP require to be carefully cleaned to make sure that the ethanol appropriately wets the internal walls of the CLPHP. Also, it stops foreign pollutants from deterioration of the working fluid through the operation of the CLPHP. The CLPHP is evacuated using a rotary vane vacuum pump, which in turn was connected with the PHP to eliminate all non-condensable gasses.

The CLPHP evaporator length was heated based on the electrical heater in a range of power input of 50 W to 450 W. The electrical power input was measured based on the electric current and voltage. The chilled water was used to cool the condenser part, which was circulated by a water pump. The heat rejected from the CLPHP was measured using thermocouples fixed at the entrance and exit of the water jacket.

Twelve K-type thermocouples (Omega Engineering Ltd.) with an accuracy of ±0.75% were fixed along the CLPHP test section length to measure the temperatures of the evaporator, adiabatic, and condenser sections, and connected to the data acquisition system. To measure the cooling water temperature, two thermocouples were fixed at the inlet and outlet of the water jacket. The water flow rate was measured using a glass-type flowmeter (LZS-15) with a needle valve to deliver a constant flow rate with an accuracy of ±4%. The supplied heat flux in terms is adjusted manually at the wanted rate using a Variac (i.e., variable AC transformer) model of (TDGC2- 1K 1000VA Single phase) with a resolution of 0.1 V and accuracy of ±0.8%. A multi-meter model of DT2700 DIGITAL was used to measure the current provided to the heater with an accuracy of ±3.0% and a resolution of 0.01 A. A high-speed data acquisition system model of USB-2416 DAQ was used to record the collected data in terms of temperatures. The vacuum pump (one-stage) model of VE115N was used to evacuate the PHP. The thermocouples were connected with data acquisition. A true angle finder (TCL) was used to measure the tilt angle of the PHP relative to the horizontal position with an accuracy of 0.5°.

Figure 2. A photograph of the developed test rig

2.3 Data processing and experimental calculation

The thermal resistance in the PHP can be defined as a key parameter of the heat transfer performance which is obtained from Eq. (2):

$$R = \frac{T_{e,av} - T_{c,av}}{Q_{in}} \tag{2}$$

The actual input power rate can be calculated by Eq. (3):

$$Q_{in} = I.V + Q_{loss} \tag{3}$$

The dissipation rate of heat in terms of heat loss, which can be calculated as following:

$$Q_{loss} = Q_{conv} + Q_{rad} \tag{4}$$

The average temperature of the evaporator and condenser can be obtained using Eq. (5):

$$T_{av} = \frac{1}{N}\sum_{i=1}^{N} T_i \tag{5}$$

The effective thermal conductivity of the PHP is calculated based on the conduction heat transfer from the evaporator to the condenser as in Eq. (6):

$$k_{eff} = \frac{L_{eff}}{A \times R} \tag{6}$$

2.4 Uncertainty analysis

The measurement uncertainty can be defined as the deviation degree between measured and actual values. Smaller uncertainty provides a more trustable measurement. Therefore, uncertainty analysis is critical in the experimental tests to demonstrate the reliability of the experimental data and results. The standard uncertainty in the input power rate and thermal resistance can be presented in the following equations, respectively.

$$\frac{\delta Q_{in}}{Q_{in}} = \sqrt{\left(\frac{dI}{I}\right)^2 + \left(\frac{dV}{V}\right)^2} \tag{7}$$

$$\frac{\delta R}{R} = \sqrt{\left(\frac{\delta T_e}{T_e - T_c}\right)^2 + \left(\frac{\delta T_c}{T_e - T_c}\right)^2 + \left(\frac{\delta Q_{in}}{Q_{in}}\right)^2} \tag{8}$$

The maximum uncertainties in the measurement and derived quantities are listed in Table 2.

Table 2. Uncertainty values in the measured quantities

Quantity	Uncertainty
Current	±0.01A
Voltage	±0.1 V
Temperature	±0.4 ºC
Flow of cooling water	±5 ml
Filling volume	±4%
Input power rate	3.79%
Thermal resistance	±4.53%

3. RESULTS AND DISCUSSION

To investigate the thermal performance of the CLPHP, the experiments were carried out in terms of the most important parameters as the start-up conditions, input power, tilt angles, thermal resistance, and effective thermal conductivity.

It is vital to show the temperature change with time to demonstrate the variation in the temperature fluctuation and the primary incidence of the geyser-boiling for each power input and tilt angle. Figure 3 shows the surface temperature change with time along the wall surface of the CLPHP at four different power inputs, vertical position (i.e., a title angle of 90°), fill ration of 0.5, and coolant inlet temperature of 20℃. It can be detected that there is no geyser boiling occurrence at a power input of 50 W, as displayed in Figure 3a. It is also observed that the temperatures of Te3 at a power input of 450 W (Figure 3d) exhibited the highest temperature readings compared with other thermocouples, then increased significantly to become the highest compared with other readings.

The basis for selecting the change in the input power values is the least power that the PHP can sense, which is 50 W. Moreover, the input power values are graded according to the output power (i.e., capacity) available in the Variac, and the difference between one value of the input power and another should be appreciable to change the temperature in each part of the PHP. Increasing the input power leads to an increase in the heat transfer through the wall of the PHP into the working fluid inside the heat pipe until it reaches the startup, after which the flow stabilizes. This means that the change in the two forms is the result of the increase in the input power. Also, the heat is transferred based on the phase change of the working substance inside the PHP. Where it is operated over a broad range of input power by selecting suitable working fluids. The changes in Figures 3c, d are due to the increase in the input power.

It may be difficult to present the temperature change for each tilt angle because of the large number of figures. Thus, the results of the variation of average temperature with time at angles of 0°, 15°, 30°, 45°, and 90° are presented in Figure 4. However, the temperature oscillation is higher for tilt angle of 0° compared with that at tilt angles of 15°, 30°, 45°, and 90°. This is because of the geyser boiling phenomena at a tilt angle of 0°, which has less effect. Therefore, a lower evaporator temperature is achieved at 30° and 45° compared with other angles. Also, it can be observed that the temperature

distribution is more uniform after the incidence of the geysering.

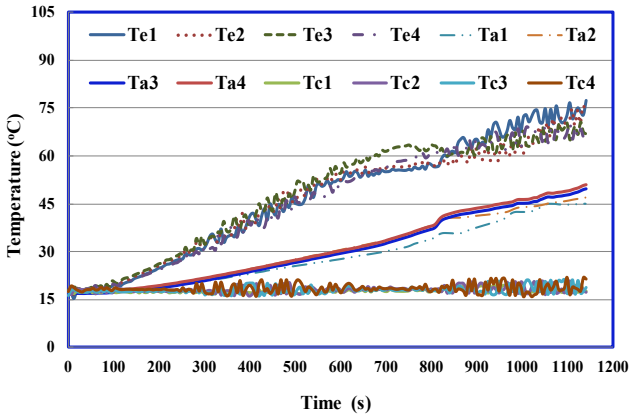

(a) Q_{in} = 50W

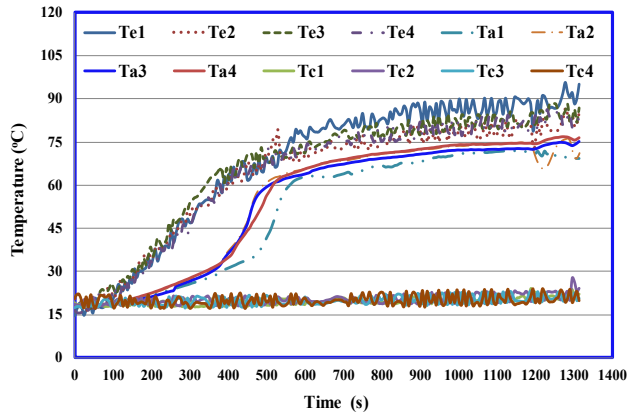

(b) Q_{in} = 115W

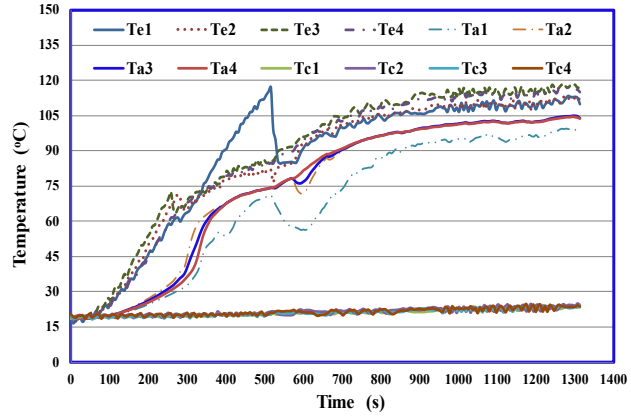

(c) Q_{in} = 215 W

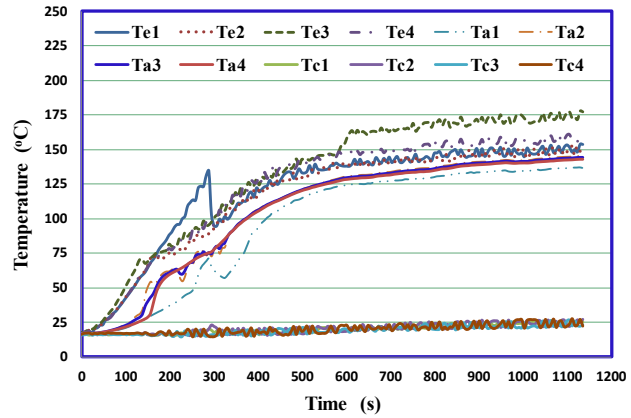

(d) Q_{in} = 450 W

Figure 3. Time dependent wall temperature at vertical orientation (θ=90°) at various power inputs

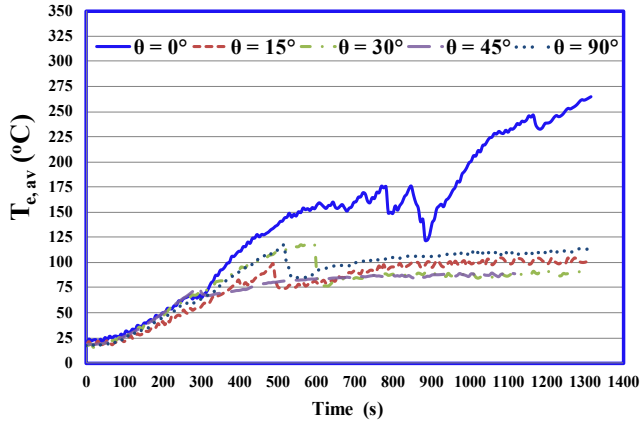

Figure 4. Average time dependent evaporator wall temperature for power input of 215 W at various tilt angles

The thermal resistance variation through the CLPHP operating with power input for four different tilt angles is shown in Figure 5. It showed that that the tilt angle of 90° (i.e., vertical position) exhibits the lowest thermal resistance for all power input due to the incidence of the geyser-boiling. It is also observed that the thermal resistance of the CLPHP in a horizontal position (i.e., tilt angle of 0°) is the highest compared with other positions because the geysering almost disappears. However, a substantial decrease in the thermal resistance after the incidence of the geyser influence was noticed at tilt angles of 45° and 90°. Also, similar trends were obtained in the average time-dependent evaporator wall temperature for the other three power inputs (i.e., 50 W, 115 W, and 450 W) at various tilt angles.

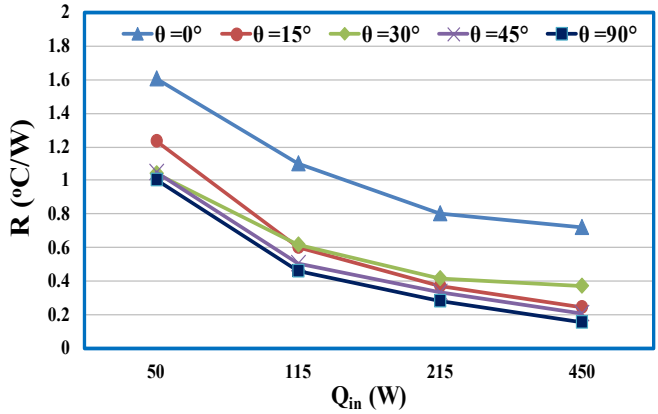

Figure 5. Variant of thermal resistance with power input at Five different tilt angles

The effective thermal conductivity affects the operation of the CLPHP, which can be considered, as one of the key effective parameters. In Figure 6, the effective thermal conductivity is presented as a function of the power input and orientations. At all tilt angles considered, the effective thermal conductivity increased when the power is increased. The best value of the effective thermal conductivity is achieved at vertical orientation and power input of 450 W, where the effective thermal conductivity increased with decreasing the tilt angle. The reason behind increasing the effective thermal resistance at high power input is that the upper part of the evaporator is repetitively covered with the warm liquid because of a higher height of the liquid phase. Also, the maximum effective conductivity is obtained at a power input

of 450 W because the dry-out did not occur in this case with a sufficient quantity of the working fluid in terms of filling ratio in the pool boiling.

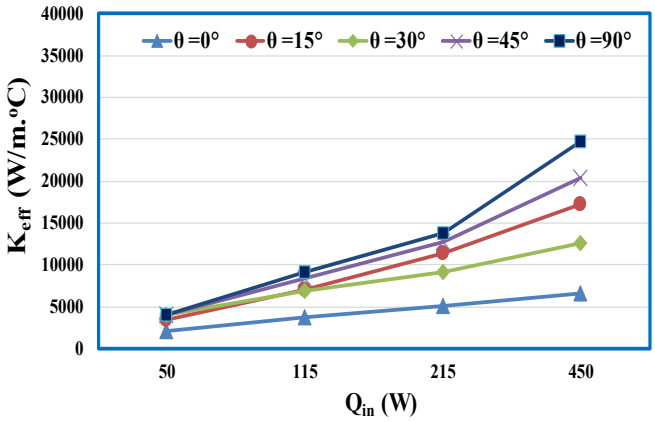

Figure 6. Variant of effective thermal conductivity with power input at Five different tilt angles

The change of the average wall surface temperature of the evaporator section as a function of a power input at a tilt angle of 45° is displayed in Figure 7. It can be seen that there is a noticeable variation in the evaporator wall temperature. This may be attributed that the liquid-phase in the evaporator section is not in touching base at specified parts of the evaporator wall because of the orientations leading to a rise in the evaporator wall temperature. Consequently, a vapor film is formed on the upper sector of the evaporator wall, which produces to further rise in the evaporator wall temperature.

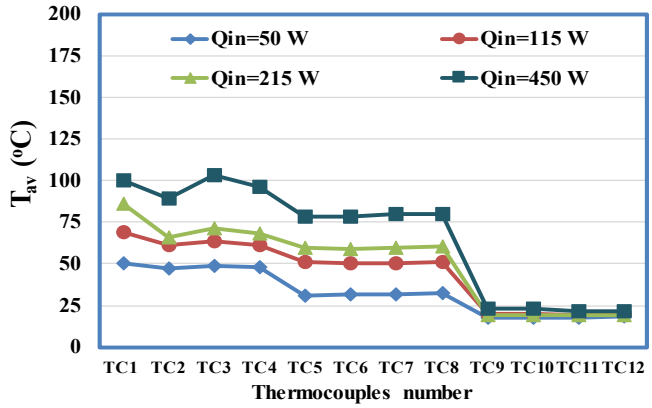

Figure 7. Variation of average temperature along the CLPHP at tilt angle of 45°

The difference between the average evaporator and condenser temperatures is shown in Figure 8. The difference between the average temperature of the evaporator and condenser decreases as the orientation increases. For a higher power input, the variation in the average temperature with the tilt angles be influenced by a power input at which the geyser influence arises. Generally, geyser-boiling arises at a higher power input as the tilt angle increases (i.e., more inclination toward the vertical orientation). Gravity plays a role in the operation of PHP. Moreover, in the horizontal position (i.e., 0° tilt angle) of PHP operation, it is hard to obtain any bubble movement. It means that the gravity force is ineffective as all the bubbles' movement should be driven by the pressure forces. Where the temperature difference between evaporator and condenser section creates those forces. Therefore, no impact was noticed in horizontal inclination. Also, the working fluid flow resistance is bulky when the PHP is started up, which leads to a slower start-up.

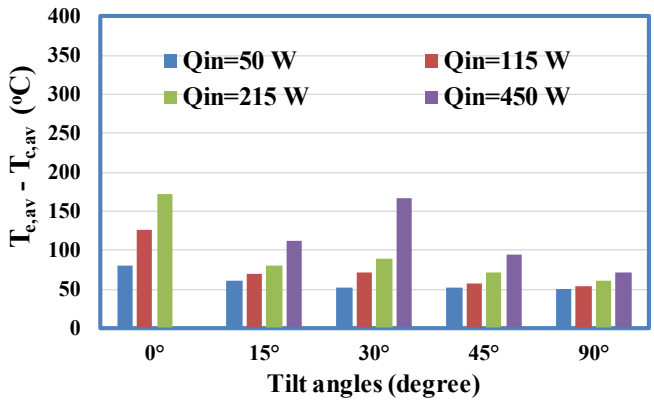

Figure 8. Average temperature difference between evaporator and condenser sections as a function of tilt angles and power input

4. CONCLUSION

In the few past years, the hot issue in the global scenario is energy management, where heat transferring devices should consume less energy in the thermal process; and need to be eco-friendly. The current study aimed to experimentally investigate the constructed CLPHP thermal performance operating with ethanol as a working fluid with a filling ratio of 0.5. Using CLPHP can also remove several weaknesses associated with the operation of conventional heat transfer devices. Consequently, enhancing the performance of CLPHP is vital to aim to enhance the performance of the thermal systems. The thermal performance of the CLPHP was investigated under various orientations (i.e., inclination angles of 0°, 15°, 30°, 45°, and 90°) and power input of 50, 115, 215, and 450 W.

The average wall temperature of the PHP decreased considerably after the geysering incidence regardless of the rise in the power input. This drop was significantly impacted by tilt angles. The best thermal performance in terms of minimum thermal resistance of 0.1585 °C/W was achieved at vertical orientation (i.e., θ=90°) and power input of 450 W. However, the thermal resistance became the lowest once the geyser boiling occurrence. The drop rate in the thermal resistance differs as the inclination and power input vary. The obtained results allow the user to categorize the range of effective conditions, that can also enhance the CLPHP performance or to avert the operating conditions leading to the adverse influence. Finally, a computational fluid dynamics model integrated with optimization technique will be developed and applied to this PHP configuration to enhance its thermal performance under different operating conditions and mixtures of the working fluids.

REFERENCES

[1] Jahanbakhsh, A., Haghgou, H.R., Alizadeh, S. (2015). Experimental analysis of a heat pipe operated solar collector using water–ethanol solution as the working

fluid. Solar Energy, 118: 267-275. https://doi.org/10.1016/j.solener.2015.04.023
[2] Ersöz, M.A. (2016). Effects of different working fluid use on the energy and exergy performance for evacuated tube solar collector with thermosyphon heat pipe. Renewable Energy, 96: 244-256. https://doi.org/10.1016/j.renene.2016.04.058
[3] Li, F., Gao, J., Shi, X., Liang, F., Zhu, K., Li, Y. (2018). Experimental investigation of an R600a two-phase loop thermosiphon to cool a motorized spindle shaft. International Communications in Heat and Mass Transfer, 97: 9-16. https://doi.org/10.1016/j.icheatmasstransfer.2018.06.005
[4] Mahdavi, M., Tiari, S., De Schampheleire, S., Qiu, S. (2018). Experimental study of the thermal characteristics of a heat pipe. Experimental Thermal and Fluid Science, 93: 292-304. https://doi.org/10.1016/j.expthermflusci.2018.01.003
[5] Su, Q., Chang, S., Song, M., Zhao, Y., Dang, C. (2019). An experimental study on the heat transfer performance of a loop heat pipe system with ethanol-water mixture as working fluid for aircraft anti-icing. International Journal of Heat and Mass Transfer, 139: 280-292. https://doi.org/10.1016/j.ijheatmasstransfer.2019.05.015
[6] Ahmed, I.S., Al Jubori, A.M. (2021). Assessment of heat transfer and flow characteristics of a two-phase closed thermosiphon. Heat Transfer, 50(2): 1351-1370. https://doi.org/10.1002/htj.21933
[7] Yao, H., Yue, C., Wang, Y., Chen, H., Zhu, Y. (2021). Numerical investigation of the heat and mass transfer performance of a two-phase closed thermosiphon based on a modified CFD model. Case Studies in Thermal Engineering, 26: 101155. https://doi.org/10.1016/j.csite.2021.101155
[8] Dai, X., Tang, Y., Liu, T., Wang, S. (2020). Experimental investigation on the thermal characteristics of ultra-thin flattened heat pipes with bending angles. Applied Thermal Engineering, 172: 115150. https://doi.org/10.1016/j.applthermaleng.2020.115150
[9] Huminic, G., Huminic, A., Fleaca, C., Dumitrache, F. (2016). Heat transfer characteristics of a two-phase closed thermosyphons using nanofluids based on sic nanoparticles. International Journal of Heat and Technology, 34: S199-S204. https://doi.org/10.18280/ijht.34S202
[10] Xu, R., Zhang, C., Chen, H., Wu, Q., Wang, R. (2019). Heat transfer performance of pulsating heat pipe with zeotropic immiscible binary mixtures. International Journal of Heat and Mass Transfer, 137: 31-41. https://doi.org/10.1016/j.ijheatmasstransfer.2019.03.070
[11] Xu, Y., Xue, Y., Qi, H. Cai, W. (2020). Experimental study on heat transfer performance of pulsating heat pipes with hybrid working fluids. International Journal of Heat and Mass Transfer, 157: 119727. https://doi.org/10.1016/j.ijheatmasstransfer.2020.119727
[12] Kim, J., Kim, S.J. (2020). Experimental investigation on working fluid selection in a micro pulsating heat pipe. Energy Conversion and Management, 205: 112462. https://doi.org/10.1016/j.enconman.2019.112462
[13] Han, H., Cui, X., Zhu, Y., Xu, T., Sui, Y., Sun, S. (2016). Experimental study on a closed-loop pulsating heat pipe (CLPHP) charged with water-based binary zeotropes and the corresponding pure fluids. Energy, 109: 724-736. https://doi.org/10.1016/j.energy.2016.05.061
[14] Perna, R., Abela, M., Mameli, M., Mariotti, A., Pietrasanta, L., Marengo, M., Filippeschi, S. (2020). Flow characterization of a pulsating heat pipe through the wavelet analysis of pressure signals. Applied Thermal Engineering, 171(10): 115128. https://doi.org/10.1016/j.applthermaleng.2020.115128
[15] Wu, Z., Xing, Y., Liu, L., Huang, P., Zhao, G. (2020). Design, fabrication and performance evaluation of pulsating heat pipe assisted tool holder. Journal of Manufacturing Processes, 50: 224-233. https://doi.org/10.1016/j.jmapro.2019.12.054
[16] Ishii, K., Fumoto, K. (2019). Temperature visualization and investigation inside evaporator of pulsating heat pipe using temperature-sensitive paint. Applied Thermal Engineering, 155: 575-583. https://doi.org/10.1016/j.applthermaleng.2019.04.026
[17] Takawale, A., Abraham, S., Sielaff, A., Mahapatra, P.S., Pattamatta, A., Stephan, P. (2019). A comparative study of flow regimes and thermal performance between flat plate pulsating heat pipe and capillary tube pulsating heat pipe. Applied Thermal Engineering, 149: 613-624. https://doi.org/10.1016/j.applthermaleng.2018.11.119
[18] Kazemi-Beydokhti, A., Meyghani, N., Samadi, M., Hajiabadi, S.H. (2019). Surface modification of carbon nanotube: Effects on pulsating heat pipe heat transfer. Chemical Engineering Research and Design, 152(4): 30-37. https://doi.org/10.1016/j.cherd.2019.09.023
[19] Wang, J., Xie, J., Liu, X. (2020). Investigation of wettability on performance of pulsating heat pipe. International Journal of Heat and Mass Transfer, 150(2): 119354. https://doi.org/10.1016/j.ijheatmasstransfer.2020.119354
[20] Liang, C.H., He, Z., Yang, Y.W., Zeng, S. (2015). Experimental study on thermal performance of pulsating heat pipe with ethanol-acetone mixtures. International Journal of Heat and Technology, 33(4): 185-190. http://dx.doi.org/10.18280/ijht.330424
[21] Charoensawan, P., Khandekar, S., Groll, M., Terdtoon, P. (2003). Closed loop pulsating heat pipes: Part A: parametric experimental investigations. Applied thermal engineering, 23(16): 2009-2020. https://doi.org/10.1016/S1359-4311(03)00159-5
[22] Yang, H., Khandekar, S., Groll, M. (2008). Operational limit of closed loop pulsating heat pipes. Applied Thermal Engineering, 28(1): 49-59. https://doi.org/10.1016/j.applthermaleng.2007.01.033

NOMENCLATURE

A	cross-sectional area of the PHP, m^2
D_c	critical inner dimeter, m
I	current, A
k	thermal conductivity, $W.m^{-1}. K^{-1}$
L	length, m
Q_{in}	actual input power rate, W
Q_{conv}	rate of convection heat transfer, W
Q_{loss}	heat loss by radiation and convection, W
Q_{rad}	rate of radiation heat transfer, W
R	thermal resistance, °C. W^{-1}
T	temperature, °C

V	voltage, volt

Greek symbols

θ	tilt angles, degree
ρ	density, $kg.m^{-3}$
σ	surface tension, $N.m^{-1}$

Subscripts

av	average
c	condenser
e	evaporator
eff	effective
l	Liquid
v	vapor